Structure and properties of hydroxyapatite for biomedical applications

1

K. Lin, J. Chang
Shanghai Institute of Ceramics, Chinese Academy of Sciences, Shanghai, China

1.1 Introduction: key properties

Hydroxyapatite (HAp) materials have drawn great interest from researchers because they are widely applied as biomedical materials, including such uses as bone fillers (Valletregi, 2004; Dorozhkin, 2009a; Xia et al., 2013), bone tissue engineering scaffolds (Dorozhkin, 2009b), bioactive coatings (Valletregi, 2004), soft tissue repairs (Okabayashi et al., 2009; Shin et al., 1992; Ji et al., 2012; Liu et al., 2012a), drug/protein/gene loading and delivery systems (Uskokovic and Uskokovic, 2011; Rodriguez-Ruiz et al., 2013; Lin et al., 2013a,b, 2011a; Zhu et al., 2004; Li et al., 2010), and column chromatography for rapid fractionation of biomolecules (Hilbrig and Freitag, 2012; Morrison et al., 2011) because of their excellent biocompatibility, osteoconductive properties, and similarity to the inorganic component of human bones (Dorozhkin, 2009b). HAp materials are also potential candidates for use in cell targeting, fluorescence labeling, imaging and diagnosis materials (Kozlova et al., 2012; Chen et al., 2012), etc. In addition, HAp is also exploited as a model compound to mimic the biomineralization process (Sadat-Shojai et al., 2013; Cai and Tang, 2008; Li et al., 2008).

Pure HAp is a stoichiometric apatite phase with a Ca/P molar ratio of 1.67 the most stable calcium phosphate salt at normal temperatures and pH between 4 and 12 (Koutsopoulos, 2002). The crystal structure of HAp most frequently encountered is hexagonal, having the $P6_3/m$ space group symmetry with lattice parameters of $a = b = 9.432$, $c = 6.881$ Å, and $\gamma = 120°$. The structure consists of an array of PO_4 tetrahedra held together by Ca ions interspersed among them. The Ca ions occur in two markedly different sites, in accurately aligned columns (Ca(I)) and in axes, and the adjacent OHs point in opposite directions (Ma and Liu, 2009). In the $P6_3/m$ form, the unit cells of HAp are arranged along the c-axis. This would justify a preferred orientation that gives rise to an oriented growth along the c-axis and a needle-like morphology (Valletregi, 2004). HAp can also exist in another form, i.e., the monoclinic form with space group $P2_1/b$ and lattice parameters $a = 9.4214(8)$, $b = 2a$, $c = 6.8814(7)$ Å, $\gamma = 120°$. The major difference between the monoclinic and hexagonal HAp is the orientations of the hydroxyl groups (OHs). In monoclinic HAp, all of OHs in a given column are pointed in the same direction, and the direction reverses in the next

Hydroxyapatite (HAp) for Biomedical Applications. http://dx.doi.org/10.1016/B978-1-78242-033-0.00001-8

column, while in hexagonal HAp the adjacent OHs point in opposite directions as mentioned above (Ma and Liu, 2009). The hexagonal HAp is usually formed by precipitation from supersaturated solutions at 25–100 °C, while the monoclinic HAp is primarily formed by heating the hexagonal form at 850 °C in air and then cooling to room temperature (Marković et al., 2004).

From a chemical perspective, the composition of biological apatites and synthetic HAp greatly differs from that of stoichiometric apatitic phases due to ion substitutions. Indeed, human bone mineral is composed of non-stoichiometric nanocrystalline apatites with structural imperfections due to co-substituted essential trace elements such as Na, Mg, Zn, Sr, K, F, Cl, Si, and CO_3^{2-} in crystal lattices (Lin et al., 2011a; Gómez-Morales et al., 2013), in which the cations usually substitute part of Ca^{2+} ions in apatitic lattice and SiO_4 tetrahedra replace partly the PO_4 tetrahedra, while the anions of F^- and Cl^- occupy OH sites. As for CO_3^{2-} ions, they can occupy OH or PO_4 tetrahedra sites to form A- and B-type carbonate apatites, respectively.

HAp has two types of crystal planes with significantly different net charges, positive charges on *a* and *b* planes, and negative charges on *c* planes, respectively. Therefore, the *a* and *b* planes tend to attract the molecules with negative charge (e.g., acidic molecules), whereas the *c* planes prefer to adsorb those with positive charges (e.g., basic molecules) (Uskokovic and Uskokovic, 2011). The elongation of HAp crystals along the *c*-axis leads to a shift toward more positively charged particles with a higher specificity for adsorption of negatively charged acidic proteins (Uskokovic and Uskokovic, 2011; Kandori et al., 2009). Moreover, the pH value of the soaking medium plays a critical role on the surface charges of HAp. When HAp particles are soaked in mineral acids or bases, negative surface charge is observed in the range of pH 5–8, which becomes even stronger with further increase of pH value (Garcia Rodenas et al., 2005).

In most cases, the morphology of precipitated HAp crystals is hexagonal in shape. It is generally considered that $Ca_9(PO_4)_6$ clusters with positive charge are the growth unit of HAp crystals (Lin et al., 2011b). Usually, hexagonal HAp crystals that grow along the *c*-axis are easily obtained because of a strong bond site for $Ca_9(PO_4)_6$ cluster in [0001] direction, but not in [100] direction. In other words, *c*-surface is a predominant crystal growth facet compared to *a*- and *b*-surfaces (Lin et al., 2011b).

The chemical composition, crystallinity, size, and morphology of the HAp crystals and their aggregates play critical roles in determining their properties and potential applications (Xia et al., 2013; Lin et al., 2013a,c, 2011a,b,c, 2007; Wu et al., 2011a; Zhang et al., 2014; Shen et al., 2012). Nanoscale HAp crystals possess excellent sintering ability due to their high surface energy (Lin et al., 2012), and the HAp nano-ceramics with enhanced mechanical properties can be fabricated using HAp nano-powders as raw materials (Sadat-Shojai et al., 2013). Moreover, HAp nano-bioceramics exhibit better bioactivity and higher resorbability than those in micro-scale sizes (Sadat-Shojai et al., 2013). HAp nanoparticles can be used for cell targeting and diagnosis (Kozlova et al., 2012; Chen et al., 2012) and drug/gene delivery (Uskokovic and Uskokovic, 2011; Rodriguez-Ruiz et al., 2013; Lin et al., 2013a,b, 2011a; Zhu et al., 2004; Li et al., 2010). Moreover, the efficiency of cell targeting, drug loading, and gene transfection was remarkably influenced by sizes and

shapes of the particles. Recently, the porous/hollow HAp aggregations with hierarchical architectures possess higher drug loading and favorably controllable release properties (Lin et al., 2011c). In addition, one-dimensional (1D) shapes, including rod-like and wire-like, and the 2D sheet-like particles can be used as the mechanical reinforcement component for preparation of composite materials (Lin et al., 2011b; Shen et al., 2012; Neira et al., 2010; Lezaja et al., 2013; Choi et al., 2010; Li and Yang, 2009; Bose et al., 2009).

1.2 Strengths/weaknesses

In biomedical applications, the main strength of HAp is its excellent biocompatibility and osteoconductive properties, which have been well summarized in previous reviews (Dorozhkin, 2009b; Hong et al., 2010). In this chapter, we will focus on their weaknesses, such as low mechanical properties and biodegradation rate, deficiency in osteoinduction, the relative lower loading capacity, and absence of targeting efficiency as delivery systems, etc. Moreover, the strategies to overcome the weaknesses will be summarized and proposed.

1.2.1 Weaknesses: low mechanical properties

HAp bioceramics are usually implanted in the form of granules and porous scaffolds. However, the major limitation to use HAp as load-bearing biomaterials are their mechanical properties, especially for macroporous scaffolds (Lin et al., 2012). So far, it is still a great challenge to improve the mechanical properties of HAp materials. The application of Al_2O_3, ZrO_2, TiO_2, metals, and carbon nanotubes, etc., as reinforcement components is the most common method to solve this problem (Mukherjee et al., 2014; Mobasherpour et al., 2009). However, most of these reinforcement components are bioinert and/or non-biocompatible, which might apparently decrease the bioactivity and biocompatibility. Compared with other materials, HAp whiskers/fibers are considered as ideal reinforcement components for HAp due to their excellent bioactivity and biocompatibility (Bose et al., 2009; Suchanek et al., 1997). However, HAp whiskers possess relatively low chemical durability in the sintering process and disappear after sintering (Lin et al., 2012).

Fabrication of HAp nano-bioceramics is another effective choice to enhance their mechanical properties, since the nano-sized ceramics exhibit apparently higher mechanical properties compared with micro-sized ceramics (Wang and Shaw, 2009). Effective suppression of accelerated grain growth is critical for the fabrication of nano-ceramics, in which lower sintering temperature, faster calcination rate, and shorter sintering time are always needed. The Spark Plasma Sintering and microwave sintering technologies are widely applied in the fabrication of nano-ceramics due to their highly efficient and rapid sintering process (Lin et al., 2012; Li et al., 2009). Lin et al. (2012) applied a simple and low-cost approach called two-step sintering (TSS)

technology to fabricate fully dense HAp nano-bioceramics using normal ovens. Compared with the conventional sintering process, the hardness (4.86 GPa) and fracture toughness (1.18 $MPa \cdot m^{1/2}$) of the dense samples fabricated by TSS were increased about 12% and 57%, respectively.

Up to now, the mechanical strength of pure HAp bioceramics obtained by various technologies is still lower than that of natural bones. Miao et al. (2007) fabricated the materials with large macropore sizes (300–500 μm), and compressive strength of 5.3–36.8 MPa and Young's moduli of 0.30–2.25 GPa by coating HAp layer on the surfaces of the interconnective macroporous ZrO_2 ceramic scaffolds. The mechanical properties and structure were similar to those of cancellous bone. However, considering the application of implant materials in load bearing place, the mechanical strength of HAp ceramics is still too low. Therefore, HAp ceramics are often coated as a thin layer on metal materials to increase the biocompatibility and osteoconductivity of the dental and orthopedic implants (Surmenev et al., 2014).

1.2.2 Weaknesses: low degradation rate

As the most stable calcium phosphate salt, artificial HAp bioceramics are difficult to be resorbed in the physiological environment, which has hindered their applications as bone grafts, tissue engineering scaffolds, drug carriers, and other applications requiring good degradability. Using a second phase with a faster degradation rate as the composite component, e.g., tricalcium phosphate, calcium carbonate, calcium sulfate, bioglass, silicate, etc., is considered as a simple method to regulate the degradation rate of HAp-based materials, and the degradability increases with the increase of additive amount (Queiroz et al., 2003; Lin et al., 2011d; Wang et al., 2013). The synthesis of calcium-deficient HAp (CHAp), amorphous HAp, and poorly crystalline HAp have attracted attention due to their good degradation ability (Mavropoulos et al., 2003; Tadic et al., 2002; Dorozhkin, 2010).

Ion substitution can lead to structural disorder and result in higher solubility, in which CO_3^{2-} substitution has revealed the most significant effect on degradation rate of the materials (Lin et al., 2011a; Zhang et al., 2014; Porter et al., 2003). Recently, our study showed that the degradation rate of HAp with co-substituted essential trace elements (Na, Mg, K, F, Cl, and CO_3^{2-}) of natural bone was about three times higher than that of pure HAp material (Lin et al., 2011a), and the dissolution rate of HAp increased with the increase of the ion substitution degree (Zhang et al., 2014; Porter et al., 2003).

In addition, the crystal grain size can also regulate the degradation rate. Comparing with micro-sized HAp bioceramics, nano-sized samples possess higher dissolution rates (Sun et al., 2007). The main degradation mechanism of apatites is solution dissolution, and the dissolution always occurs most easily on grain boundaries. Nano-sized HAp bioceramics possess much more boundaries, which lead to higher dissolution rate (Lin et al., 2011e). Indeed, the low crystallinity, ion substitution, and small crystal size (~50 nm in length, 25 nm in width, and 2–5 nm in thicknesses) of natural apatite are very important factors that are related to their good solubility (Valletregi, 2004).

1.2.3 Weaknesses: lack of osteoinductivity

Though HAp bioceramics possess good biocompatibility and high osteoconductivity, traditional artificial HAp bioceramics are still generally considered to lack sufficient bioactivity and osteoinductivity to induce osteogenic differentiation of the stem cells and osteoblasts and to stimulate new bone formation, which is essential for regeneration of large bone defects, senile bone regeneration, and bone tissue engineering (Lin et al., 2013c; Zhang et al., 2014).

The chemical composition and surface morphology design are considered as potent approaches to improve the bioactivity and biological responses of the grafts (Xia et al., 2013; Lin et al., 2011a, 2013c). Indeed, the biological apatites are always co-substituted by essential trace elements on trace levels. Comprehensive studies have revealed that these substitutions play important roles in the biological performance of apatites (Lin et al., 2013a, 2011a,b; Zhang et al., 2014). For example, Na plays a significant role in bone metabolism and osteoporosis; Mg has an important role in calcified tissues and indirectly influences mineral metabolism; K is an active element in mineralization and biochemical processes; F has been well recognized for its potential effect on the prevention of dental decay and enhancement of mineralization and crystallization of calcium phosphates in bone formation; Cl enables an acidic environment to develop on the surface of bone that activates osteoclasts in the bone resorption process; the incorporation of CO_3^{2-} ions has advantages for excellent biocompatibility and resorbability of ion-substituted HAp; and Si plays a critical role in the normal bone, cartilage, and connective tissue growth and development by promoting collagen type I synthesis, osteoblast differentiation, and bone repair (Lin et al., 2011a; Zhang et al., 2014). In addition, the incorporation of Si into HAp has been shown to significantly increase the rate of bone apposition to HAp bioceramic implants (Porter et al., 2003). As for Sr, this element has been shown to have the dual effect of stimulating osteoblast differentiation and inhibiting osteoclast activity and bone resorption (Lin et al., 2013d). A large number of studies has confirmed that the incorporation of functional trace elements can significantly enhance the bioactivity of HAp bioceramics. Moreover, the incorporation of Sr ions into HAp might also stimulate expression of the angiogenic factor such as vascular endothelial growth factor (VEGF) *in vitro* (Lin et al., 2013a). The angiogenesis is extraordinarily important during bone regeneration, especially for segmental bone defect regeneration, which stimulates the diffusion of oxygen and nutrients from the surrounding tissue to ensure the viability and function of cells (Lin et al., 2013a).

Other than the functional element incorporation, the improvement of bone healing can be achieved via tailoring the surface structure of the grafts. Some studies showed that HAp bioceramics with nanoscale crystal sizes and biomimetic micro-/nano-structured topographies possess better bioactivity to promote adhesion, proliferation, and osteogenic differentiation of BMSCs and osteoblasts and to subsequently stimulate bone healing (Li et al., 2009; Sun et al., 2007; Morisue et al., 2009; Zhou and Lee, 2011). However, tailoring of the nano-/micro-structured topographies on HAp bioceramics in macroscopical size is a big challenge due to their brittleness. Recently, multilevel hierarchically ordered artificial HAp materials with biomimetic

structure in macroscopical size has been successfully constructed via hard-template precursor transformation technology using centimeter-sized α-TCP ceramics and $CaHPO_4$ single crystals as precursors (Xia et al., 2013; Lin et al., 2013c; Liu et al., 2012b, 2013). Moreover, the highly interconnective macroporous HAp scaffolds with nanosheet, nanorod, and micro-nano-hybrid (hybrid of nanorods and microrods) surface topographies have been prepared, and the surface morphology was controlled simply by regulation of the hydrothermal medium of NaH_2PO_4, Na_3PO_4, and $CaCl_2$ aqueous solution, respectively (Figure 1.1a1–d1) (Xia et al., 2013).

Compared with the HAp bioceramic flat surface (S0), HAp bioceramics with hierarchical 3D micro-nano-textured surfaces (S1–S3) possessed higher specific surface area, which enhanced selective adsorption of specific proteins in plasma and stimulated osteoblast and BMSC adhesion, growth, and osoteogenic differentiation. In particular, the biomimetic features of hierarchical micro-nano-hybrid surface result in the simultaneous enhancement of protein adsorption, stem cell proliferation, and differentiation and subsequently lead to acceleration of bone regeneration (Figure 1.1). The

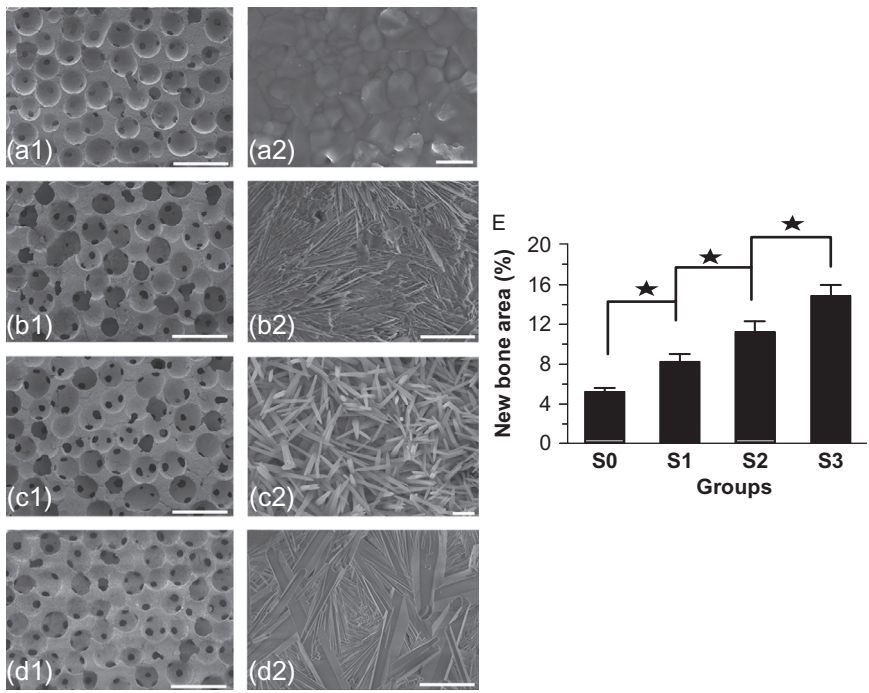

Figure 1.1 SEM micrographs of macroporous HAp ceramic scaffolds (a1–d1) and corresponding topographic surfaces of pore walls (a2–d2), such smooth surface (S0), nanosheet surface (S1), nanorod surface (S2), and micro-nano-hybrid surface (S3), respectively. The histological analysis of newly formed bone in calvarial defects after implantation of the scaffolds for 8 weeks (e). Scale bar of a1–d1 = 1 mm; scale bar of a2 and c2 = 1 μm; scale bar of b2 and d2 = 10 μm. An asterisk indicates statistically significant differences, $p < 0.05$ (Xia et al., 2013).

results suggest that the combination of micro- and nano-structured topography might need to be considered in the design of functional bone grafts (Xia et al., 2013; Lin et al., 2013c).

The addition of the growth factors (such as BMP, VEGF, and peptide) (Sawyer et al., 2005; Bose and Tarafder, 2012; Na et al., 2007; Hennessy et al., 2009) (Notodihardjo et al., 2012) and loading mesenchymal stem cells or endothelial cells (Na et al., 2007; Yu et al., 2009) are widely applied to improve the bioactivity and bone regeneration ability of the HAp bioceramics. However, the application of growth factors and stem cells demonstrate rather high batch variability and has high production costs (Yuan et al., 2010).

Kizukia et al. (2003) and Itoh et al. (2006) developed a simple electrical polarization method to improve the bioactivity of HAp bioceramics. The studies showed that electrical polarization could accelerate the adhesion and proliferation of osteoblasts and subsequently complete bone in-growth and penetration as early as 3 weeks after surgery. In contrast, non-polarized implants were not fully ossified even 6 weeks after surgery.

1.2.4 Weaknesses: lack of targeting and labeling

HAp materials have been receiving a great deal of attention in their applications as drug delivery systems. However, the relatively low drug-loading capacity and difficulty in controlling release rate, the low degradation rate, and the absence of targeting efficiency and labeling capacity are drawbacks of HAp in this application. In addition, the chemically synthesized HAp nanoparticles are usually significantly aggregated, which further limits its application, most especially in intravenous administration.

The synthesis of HAp materials with good dispersibility and small crystal size, in particular the meso-, porous, and hollow structures, can significantly improve the specific surface area and pore volume of the products, which will result in higher drug-loading capacity. Moreover, comparing with particles, meso-, porous, and hollow structures can not only provide much more space for loading drug molecules, but also facilitate the control of the release rate of the loaded drugs (Lin et al., 2013a,b, 2011c; Wu et al., 2011a; Uota et al., 2005; Ng et al., 2010), whereas the degradation rate of HAp carriers can be improved by ion substitution, reduction of the crystallinity, and introduction of calcium-deficient and amorphous phases (Lin et al., 2011a; Zhang et al., 2014; Mavropoulos et al., 2003; Tadic et al., 2002; Dorozhkin, 2010; Porter et al., 2003).

Uskokovic and Uskokovic (2011) proposed a strategy for the development of multifunctional calcium phosphate particles with targeting and labeling capacities, which might be used to design HAp composite particles with multifunctional properties for drug delivery systems. Indeed, the magnetic component of iron oxide and active targeting reagent of folic acid have been widely incorporated to overcome the problem of low targeting efficiency for HAp (Lin et al., 2013b; Guo et al., 2011; Rout et al., 2012). Hollow magnetic HAp microspheres with hierarchically mesoporous structures, high drug-loading capacity, and sustained drug release property have been synthesized via hydrothermal treatment of the similar structured $CaCO_3/Fe_3O_4$ hollow microspheres

as the sacrificial hard-templates. In addition, the magnetic properties of these biocompatible HAp microspheres could be well adjusted by modulation of Fe_3O_4 amount; the drug release rate of the microspheres is apparently affected by pH, and the decrease of the pH values of the solution medium resulted in an increase of the release rate. The results suggested that fabricated multifunctional hollow microspheres have great potential for magnetic and pH responsive drug-delivery applications (Lin et al., 2013b). On the other hand, the fluorescence labeling technology using rare earth and fluorescent dyes was introduced to overcome the labeling efficiency of HAp (Rout et al., 2012; Ashokan et al., 2010).

The surfactants, nano-reactors, and ultrafast nucleation approach are usually employed to inhibit the excess agglomeration of HAp particles. Lin et al. (2007) used novel microemulsion nano-reactors under hydrothermal condition to synthesize single-crystal HAp nanorods with mono-dispersion and narrow-size distribution, and the obtained HAp particles have the diameter of 25–40 nm. Most recently, Zou et al. (2012) developed a novel sonochemistry-assisted microwave process to synthesize HAp nanoparticles with excellent dispersibility and specific surface area around 90 m^2/g in ultra-short-period of 5 min, in which the microwave treatment rapidly stimulated the nucleation rate while the ultrasonic irradiation apparently promoted the crystallization process and increased the specific surface area as well as dispersibility of the as-obtained products.

1.3 Examples of applications

HAp material has the potential for applications in bone and tooth repair. In addition, in recent years, applications in drug-delivery systems, cell targeting, imaging and diagnosis, etc., have also been studied. Furthermore, HAp is also applied for rapid fractionation of proteins, nucleic acids, and antibodies, which will also be briefly reviewed in this section.

1.3.1 Application for hard tissue repairs

Due to its similarity with the inorganic component of human bone and teeth, HAp is considered as an ideal candidate for hard tissue repair and has been widely used in orthopedics and dentistry for nearly 40 years (Hench, 1991). In clinical practice, HAp bioceramics are usually applied in (1) powders or granules for bone and tooth defect filling; (2) particles as the component for tooth pastes and bone cements; (3) small and unloaded implants, such as in the middle ear; (4) porous scaffolds acting as temporary substrates for cell in-growth and new bone development under non-load-bearing sites; (5) biocompatible and bioactive coatings on metal implants for dental implants and hip joint prosthesis where load-bearing properties are required; or (6) the bioactive phase and mechanical reinforcement in a polymer-bioactive ceramic composite (Valletregi, 2004; Hench, 1991).

The studies show that synthetic HAp grafts usually integrate well with the surrounding host bone and promote new bone formation, leading to bonding with newly formed bone and recovery of damaged bone tissue. *In vivo* studies using rabbits showed that the graft was superior in terms of bonding with the host bone as well as induction and integration with new bone compared to the allografts and bone grafts with low HAp content (Zhou and Lee, 2011). In addition, HAp nanoparticles have been widely used as the bioactive component in fabricating biocomposite bone grafts as well as a matrix for bone tissue engineering (Cui et al., 2007).

Recently, our studies showed that the nano-/micro-structured surface of HAp bioceramics promote new bone formation and mineralization when compared with HAp with smooth surfaces. For example, after implanting the macroporous HAp bioceramic scaffolds in rat critical-sized calvarial defect for 8 weeks, the percentage of new bone area formed in HAp bioceramic scaffolds with smooth surface, nanosheet surface, nanorod surface, and micro-nano-hybrid surface of the pore walls was $5.08 \pm 1.09\%$, $8.17 \pm 1.62\%$, $11.13 \pm 2.38\%$, and $14.79 \pm 2.22\%$, respectively. This result suggests that the hierarchical micro-nano-hybrid topography might be one of the critical factors to be considered in the design of functional bone grafts (Xia et al., 2013; Lin et al., 2013c). In addition, the biological responses including the cell adhesion and spreading, proliferation and differentiation, and bone regeneration are closely related to the porosity and micropore size, crystal shape and size, crystallinity, and ion-substitution of the HAp materials (Zhou et al., 2013; Hu et al., 2007).

The enamel is mainly composed of about 97 wt.% needle-like apatite nanocrystals, which are bundled in parallel ordered prisms to ensure unique mechanical strength and biological protection (Dorozhkin, 2009b). Moreover, enamel is infrequently self-repaired by living organisms after substantial mineral loss (Dorozhkin, 2009b). The study of Tang et al. (Li et al., 2008) suggested that 20-nm-sized HAp is a better candidate than any restorative material used to date to perfectly repair eroded enamel. The nano HAp can be strongly adsorbed onto enamel surfaces to induce the remineralization of the enamel surface.

Recently, HAp nanocrystals were also recognized as an important bioactive component in facilitating cartilage regeneration (Zhou et al., 2013). Compared with pure PLGA scaffolds, the incorporation of HAp nanoparticles could apparently stimulate the adhesion and proliferation of chondrocytes and possessed better cartilage regeneration ability without using any growth factors or gene transfer (Lee et al., 2008; Xue et al., 2010). The addition of the HAp component not only improves the bioactivity, but also enhances mechanical properties in cartilage regeneration to improve anti-friction properties (Lee et al., 2008). Moreover, a 2D-shaped HAp crystal is generally considered as the most effective additive to stiffen the composite materials, while a 1D-shaped morphology is less effective but better than a sphere shape (Neira et al., 2010).

1.3.2 Application as bone tissue engineering scaffolds

The tissue engineering technology possesses the potential to solve the challenge of large-size bone defect regeneration and reconstruction of lost bone tissue. The bone tissue engineering involves the following strategies: the use of isolated cells or cell

substitutes to replace limited functions of the tissue and the utilization of tissue-inducing substances such as growth factors and scaffolds to direct tissue development (Zhou and Lee, 2011). HAp is considered as a potential candidate as a scaffold for bone tissue engineering applications, which act as a excellent temporary substrate to allow cell in-growth, proliferation, and differentiation and subsequent bone tissue regeneration after implantation *in vivo*. Therefore, one of the main issues in this field is the development of fabrication techniques to tailor surface properties of HAp scaffolds in order to control and regulate cell biological responses.

Furthermore, to better mimic the structure and biological function of native bone tissue, composite scaffolds are designed by dispersing HAp particles in biopolymer matrix, in which HAp particles function as both bioactive and mechanical reinforcing components (Zhou and Lee, 2011). For example, Kim et al. (2006) have used PLGA/HAp composite scaffolds to construct the living bone tissues *in vivo* at ectopic sites.

1.3.3 Application for soft tissue repairs

HAp materials have also garnered attention in soft tissue regeneration due to their excellent biocompatibility with soft tissues such as skin, muscle, and gums. The studies showed that the HAp can activate fibroblasts and accumulate vessel endothelial cells and thereby support the healing of skin wounds (Okabayashi et al., 2009). HAp bioceramics contact tightly and adhere strongly with skin tissue to prevent exit-site and tunnel bacterial infection, which suggests that HAp materials might be utilized as percutaneous devices (Shin et al., 1992). The composite products with a HAp component have been successfully developed for soft-tissue augmentation (Ji et al., 2012), and a study has demonstrated that HAp nanoparticles could stimulate the axonal out-growth, suggesting that HAp might provide a new approach for therapy or prevention of nerve injury (Liu et al., 2012a).

1.3.4 Application as drug/gene/protein carriers

HAp materials can serve as carriers for drug/protein delivery and gene therapy due to their excellent biocompatibility, easily tunable physical–chemical properties (e.g., size, morphology, porous structure, and surface composition), low toxicity, low production cost, excellent storage stability, inertia to microbial degradation, and pH-dependent dissolution, etc. (Rodriguez–Ruiz et al., 2013; Lin et al., 2013a,b, 2011a,c; Zhu et al., 2004; Li et al., 2010; Wu et al., 2011a,b; Uota et al., 2005; Ng et al., 2010; Kundu et al., 2013). With the decrease of the pH value from alkaline to acidic conditions, the degradation rate of HAp increases apparently, which accelerates the release of the drug molecules from the HAp surfaces. The feature of the pH-dependent dissolution property is particularly interesting since pH of about 7.4 is observed in normal tissues, and the values of about 5 are found in extracellular environments of solid tumors, in particular within the endosome–lysosome cell compartment, which enables a preferential active drug release from HAp surface in a pH-dependent way in the tumor region (Rodriguez-Ruiz et al., 2013; Lin et al., 2013b; Kundu et al., 2013). In addition, the drug-loading amount, release properties, and therapeutic effects

are critically related to the characteristics of HAp materials, including size, shape, aspect ratio, crystallinity, chemical composition, morphology, porous structure, and surface chemistry property, etc. Furthermore, fabrication of porous-structured and 3D-architectured HAp are the most effective approaches to overcoming the disadvantages of HAp as drug carriers, such as low drug-loading capacity and faster release rate (Lin et al., 2013a,b, 2011a,c; Wu et al., 2011a,b; Uota et al., 2005; Ng et al., 2010).

1.3.5 Applications in bioimaging and diagnosis

Multi-modal molecular imaging can significantly improve the potential of non-invasive medical diagnosis by combining basic anatomical descriptions with in-depth phenotypic characteristics of disease. Most recently, the multi-modal contrast agent based on HAp nanoparticles has been reported (Chen et al., 2012; Ashokan et al., 2010), in which the incorporation of magnetic components and the modification of the particle surface with folic acid are usually adopted to bring the target property, while the rare earth elements are used for the doping of HAp to endow it with imaging and diagnosis capacities.

Ashokan et al. (2010) reported the synthesis and properties of multi-modal contrast agent based on mono-dispersed HAp particles in the size of 30 nm, which showed simultaneous contrast enhancement for three major molecular imaging techniques such as magnetic resonance imaging (MRI), X-ray imaging, and near-infrared (NIR) fluorescence imaging. In this application, the doping of HAp with Eu^{3+} (3 at %) resulted in bright NIR fluorescence (700 nm) due to efficient $^5D_0$–$^7F_4$ electronic transitions, and co-doping with Gd^{3+} resulted in enhanced paramagnetic longitudinal relaxivity ($r1 \sim 12\ mM^{-1}\ s^{-1}$) suitable for T_1-weighted MR imaging together with ~80% X-ray attenuation suitable for X-ray contrast imaging.

1.3.6 Rapid fractionation of proteins, nucleic acids, and antibodies

HAp has been applied as an adsorbent and purification agent in chromatography for separation of proteins, nucleic acids, and antibodies for more than 60 years due to their high stability, high adsorption capacity, high selectivity, resistance to biochemical degradation, and low toxicity, etc. (Hilbrig and Freitag, 2012; Morrison et al., 2011; Akkaya, 2013). For example, the immunoglobulin G (IgG) adsorption onto solid surfaces is very important for biomedical applications, such as immunoassays and biosensors (Akkaya, 2013). Akkaya fabricated a novel porous and spherical HAp microcomposite with an average diameter of 50–100 μm and high specific surface area of 182.53 m^2/g for the adsorption of human IgG. An adsorption capacity of IgG on HAp microcomposite reached a high value of 140 mg/g, and the IgG molecules could be repeatedly adsorbed and desorbed through the use of spherical microcomposites without a noticeable loss in the IgG adsorption capacity (Akkaya, 2013).

1.4 Future trends

HAp materials are widely used in hard and soft tissue repair, bone tissue engineering, drug/gene/protein delivery, chromatography, imaging, and diagnosis. The performance of HAp materials in applications depends on its chemical compositions and structures. However, there are still many open questions and challenges that need to be further investigated in detail. The future trends of HAp for biomedical applications might lie in the following aspects:

(1) The physical, chemical, and biological properties of HAp are critically related to its chemical composition and structure. So far, many strategies have been developed to control the chemical composition and structure of HAp materials to meet the requirement. However, the controlling mechanisms behind each synthesis process might be very different. The real mechanisms for controlling the chemical composition and structure need to be comprehensively researched and confirmed, which are critical for design of HAp products for different biomedical applications.

(2) Low degradation rate is one the drawback of HAp materials, which hinders its applications as bone grafts, bone tissue engineering scaffolds and degradable drug delivery materials. Therefore, deign of HAp based biomaterials with controllable degradation rate is a challenge.

(3) It is still difficult to synthesize uniform HAp particles with mono-dispersion and narrow-size distribution in a large scale, which is very important for application as drug carriers. Moreover, the development of the HAp-based nanoparticles with the integration of diagnosis and therapy capacity is one of the most important aims and challenges for future HAp applications.

(4) The fabrication of HAp materials with excellent osteoinductive properties is an important future trend because of the potential applications for regeneration of large-sized bone defect or reconstruction of lost bone tissue using bone tissue engineering technology. The functional element incorporation and nano-/macro-structured surface design will be the most effective and low-cost approaches to achieve this objective. However, how to delicately control the composition and surface topology of the materials, and the relationship between the osteoinduction and composition/surface topology need to be further investigated. This will take hard work.

References

Akkaya, B., 2013. Porous and spherical hydroxyapatite microcomposites for immunoglobulin G adsorption. J. Appl. Polym. Sci. 130, 2764–2771. http://dx.doi.org/10.1002/APP.39341.

Ashokan, A., Menon, D., Nair, S., Koyakutty, M., 2010. A molecular receptor targeted, hydroxyapatite nanocrystal based multi-modal contrast agent. Biomaterials 31, 2606–2616.

Bose, S., Tarafder, S., 2012. Calcium phosphate ceramic systems in growth factor and drug delivery for bone tissue engineering: a review. Acta Biomater. 8, 1401–1421.

Bose, S., Banerjee, A., Dasgupta, S., Bandyopadhyay, A., 2009. Synthesis, processing, mechanical, and biological property characterization of hydroxyapatite whisker-reinforced hydroxyapatite composites. J. Am. Ceram. Soc. 92, 323–330.

Cai, Y., Tang, R., 2008. Calcium phosphate nanoparticles in biomineralization and biomaterials. J. Mater. Chem. 18, 3775–3787.

Chen, F., Huang, P., Zhu, Y.J., Wu, J., Cui, D.X., 2012. Multifunctional Eu^{3+}/Gd^{3+} dual-doped calcium phosphate vesicle-like nanospheres for sustained drug release and imaging. Biomaterials 33, 6447–6455.

Choi, W.-Y., Kim, H.-E., Kim, M.-J., Kim, U.-C., Kim, J.-H., Koh, Y.-H., 2010. Production and characterization of calcium phosphate (CaP) whisker-reinforced poly(ε-caprolactone) composites as bone regenerative. Mater. Sci. Eng. C 30, 1280–1284.

Cui, F.-Z., Li, Y., Ge, J., 2007. Self-assembly of mineralized collagen composites. Mater. Sci. Eng. R. Rep. 57, 1–27.

Dorozhkin, S., 2009a. Calcium orthophosphate cements and concretes. Materials 2, 221–291.

Dorozhkin, S., 2009b. Nanodimensional and nanocrystalline apatites and other calcium orthophosphates in biomedical engineering, biology and medicine. Materials 2, 1975–2045.

Dorozhkin, S.V., 2010. Amorphous calcium (ortho)phosphates. Acta Biomater. 6, 4457–4475.

Garcia Rodenas, L., Palacios, J.M., Apella, M.C., Morando, P.J., Blesa, M.A., 2005. Surface properties of various powdered hydroxyapatites. J. Colloid Interface Sci. 290, 145–154.

Gómez-Morales, J., Iafisco, M., Delgado-López, J.M., Sarda, S., Drouet, C., 2013. Progress on the preparation of nanocrystalline apatites and surface characterization: overview of fundamental and applied aspects. Prog. Cryst. Growth Charact. Mater. 59, 1–46.

Guo, Y.-P., Guo, L.-H., Y-b, Yao, Ning, C.-Q., Guo, Y.-J., 2011. Magnetic mesoporous carbonated hydroxyapatite microspheres with hierarchical nanostructure for drug delivery systems. Chem. Commun. 47, 12215–12217.

Hench, L.L., 1991. Bioceramics: from concept to clinic. J. Am. Ceram. Soc. 74, 1487–1510.

Hennessy, K.M., Pollot, B.E., Clem, W.C., Phipps, M.C., Sawyer, A.A., Culpepper, B.K., et al., 2009. The effect of collagen I mimetic peptides on mesenchymal stem cell adhesion and differentiation, and on bone formation at hydroxyapatite surfaces. Biomaterials 30, 1898–1909.

Hilbrig, F., Freitag, R., 2012. Isolation and purification of recombinant proteins, antibodies and plasmid DNA with hydroxyapatite chromatography. Biotechnol. J. 7, 90–102.

Hong, Y., Fan, H., Li, B., Guo, B., Liu, M., Zhang, X., 2010. Fabrication, biological effects, and medical applications of calcium phosphate nanoceramics. Mater. Sci. Eng. R. Rep. 70, 225–242.

Hu, Q., Tan, Z., Liu, Y., Tao, J., Cai, Y., Zhang, M., et al., 2007. Effect of crystallinity of calcium phosphate nanoparticles on adhesion, proliferation, and differentiation of bone marrow mesenchymal stem cells. J. Mater. Chem. 17, 4690.

Itoh, S., Nakamura, S., Nakamura, M., Shinomiya, K., Yamashita, K., 2006. Enhanced bone ingrowth into hydroxyapatite with interconnected pores by Electrical Polarization. Biomaterials 27, 5572–5579.

Ji, D.-Y., Kuo, T.-F., Wu, H.-D., Yang, J.-C., Lee, S.-Y., 2012. A novel injectable chitosan/polyglutamate polyelectrolyte complex hydrogel with hydroxyapatite for soft-tissue augmentation. Carbohydr. Polym. 89, 1123–1130.

Kandori, K., Oda, S., Fukusumi, M., Morisada, Y., 2009. Synthesis of positively charged calcium hydroxyapatite nano-crystals and their adsorption behavior of proteins. Colloids Surf. B Biointerfaces 73, 140–145.

Kim, S.S., Sun Park, M., Jeon, O., Yong Choi, C., Kim, B.S., 2006. Poly(lactide-co-glycolide)/hydroxyapatite composite scaffolds for bone tissue engineering. Biomaterials 27, 1399–1409.

Kizukia, T., Ohgaki, M., Katsura, M., Nakamura, S., Hashimoto, K., Toda, Y., et al., 2003. Effect of bone-like layer growth from culture medium on adherence of osteoblast-like cells. Biomaterials 24, 941–947.

Koutsopoulos, S., 2002. Synthesis and characterization of hydroxyapatite crystals: a review study on the analytical methods. J. Biomed. Mater. Res. 62, 600–612.

Kozlova, D., Chernousova, S., Knuschke, T., Buer, J., Westendorf, A.M., Epple, M., 2012. Cell targeting by antibody-functionalized calcium phosphate nanoparticles. J. Mater. Chem. 22, 396–404.

Kundu, B., Ghosh, D., Sinha, M.K., Sen, P.S., Balla, V.K., Das, N., et al., 2013. Doxorubicin-intercalated nano-hydroxyapatite drug-delivery system for liver cancer: an animal model. Ceram. Int. 39, 9557–9566.

Lee, J.B., Lee, S.H., Yu, S.M., Park, J.-C., Choi, J.B., Kim, J.K., 2008. PLGA scaffold incorporated with hydroxyapatite for cartilage regeneration. Surf. Coat. Technol. 202, 5757–5761.

Lezaja, M., Veljovic, D.N., Jokic, B.M., Cvijovic-Alagic, I., Zrilic, M.M., Miletic, V., 2013. Effect of hydroxyapatite spheres, whiskers, and nanoparticles on mechanical properties of a model BisGMA/TEGDMA composite initially and after storage. J. Biomed. Mater. Res. B Appl. Biomater. 101, 1469–1476.

Li, L., Yang, G., 2009. Synthesis and properties of hydroxyapatite nanorod-reinforced polyamide 6 nanocomposites. Polym. Int. 58, 380–387.

Li, L., Pan, H., Tao, J., Xu, X., Mao, C., Gu, X., et al., 2008. Repair of enamel by using hydroxyapatite nanoparticles as the building blocks. J. Mater. Chem. 18, 4079–4084.

Li, B., Chen, X., Guo, B., Wang, X., Fan, H., Zhang, X., 2009. Fabrication and cellular biocompatibility of porous carbonated biphasic calcium phosphate ceramics with a nanostructure. Acta Biomater. 5, 134–143.

Li, J., Chen, Y.C., Tseng, Y.C., Mozumdar, S., Huang, L., 2010. Biodegradable calcium phosphate nanoparticle with lipid coating for systemic siRNA delivery. J. Control. Release 142, 416–421.

Lin, K., Chang, J., Cheng, R., Ruan, M., 2007. Hydrothermal microemulsion synthesis of stoichiometric single crystal hydroxyapatite nanorods with mono-dispersion and narrow-size distribution. Mater. Lett. 61, 1683–1687.

Lin, K., Zhou, Y., Zhou, Y., Qu, H., Chen, F., Zhu, Y., et al., 2011a. Biomimetic hydroxyapatite porous microspheres with co-substituted essential trace elements: surfactant-free hydrothermal synthesis, enhanced degradation and drug release. J. Mater. Chem. 21, 16558–16565.

Lin, K., Chang, J., Liu, X., Chen, L., Zhou, Y., 2011b. Synthesis of element-substituted hydroxyapatite with controllable morphology and chemical composition using calcium silicate as precursor. CrystEngComm 13, 4850–4855.

Lin, K., Liu, X., Chang, J., Zhu, Y., 2011c. Facile synthesis of hydroxyapatite nanoparticles, nanowires and hollow nano-structured microspheres using similar structured hard-precursors. Nanoscale 3, 3052–3055.

Lin, K., Zhang, M., Zhai, W., Qu, H., Chang, J., 2011d. Fabrication and characterization of hydroxyapatite/wollastonite composite bioceramics with controllable properties for hard tissue repair. J. Am. Ceram. Soc. 94, 99–105.

Lin, K., Yuan, W., Wang, L., Lu, J., Chen, L., Wang, Z., et al., 2011e. Evaluation of host inflammatory responses of beta-tricalcium phosphate bioceramics caused by calcium pyrophosphate impurity using a subcutaneous model. J. Biomed. Mater. Res. B Appl. Biomater. 99, 350–358.

Lin, K., Chen, L., Chang, J., 2012. Fabrication of dense hydroxyapatite nanobioceramics with enhanced mechanical properties via two-step sintering process. Int. J. Appl. Ceram. Technol. 9, 479–485.

Lin, K., Liu, P., Wei, L., Zou, Z., Zhang, W., Qian, Y., et al., 2013a. Strontium substituted hydroxyapatite porous microspheres: surfactant-free hydrothermal synthesis, enhanced biological response and sustained drug release. Chem. Eng. J. 222, 49–59.

Lin, K., Chen, L., Liu, P., Zou, Z., Zhang, M., Shen, Y., et al., 2013b. Hollow magnetic hydroxyapatite microspheres with hierarchically mesoporous microstructure for pH-responsive drug delivery. CrystEngComm 15, 2999–3008.

Lin, K., Xia, L., Gan, J., Zhang, Z., Chen, H., Jiang, X., et al., 2013c. Tailoring the nanostructured surfaces of hydroxyapatite bioceramics to promote protein adsorption, osteoblast growth, and osteogenic differentiation. ACS Appl. Mater. Interfaces 5, 8008–8017.

Lin, K., Xia, L., Li, H., Jiang, X., Pan, H., Xu, Y., et al., 2013d. Enhanced osteoporotic bone regeneration by strontium-substituted calcium silicate bioactive ceramics. Biomaterials 34, 10028–10042.

Liu, M., Zhou, G., Song, W., Li, P., Liu, H., Niu, X., et al., 2012a. Effect of nano-hydroxyapatite on the axonal guidance growth of rat cortical neurons. Nanoscale 4, 3201–3207.

Liu, X., Lin, K., Qian, R., Chen, L., Zhuo, S., Chang, J., 2012b. Growth of highly oriented hydroxyapatite arrays tuned by quercetin. Chem. Eur. J. 18, 5519–5523.

Liu, X., Lin, K., Wu, C., Wang, Y., Zou, Z., Chang, J., 2013. Multilevel hierarchically ordered artificial biomineral. Small 10, 152–159.

Ma, G., Liu, X., 2009. Hydroxyapatite: hexagonal or monoclinic. Cryst. Growth Des. 9, 2991–2994.

Marković, S., Fowler, B.O., Tung, M.S., 2004. Preparation and comprehensive characterization of calicum hydroxyapatite reference material. J. Res. Natl. Inst. Stand. Technol. 109, 553–568.

Mavropoulos, E., Rossi, A.M., da Rocha, N.C.C., Soares, G.A., Moreira, J.C., Moure, G.T., 2003. Dissolution of calcium-deficient hydroxyapatite synthesized at different conditions. Mater. Charact. 50, 203–207.

Miao, X., Hu, Y., Liu, J., Huang, X., 2007. Hydroxyapatite coating on porous zirconia. Mater. Sci. Eng. C 27, 257–261.

Mobasherpour, I., Solati Hashjin, M., Razavi Toosi, S.S., Darvishi Kamachali, R., 2009. Effect of the addition ZrO_2–Al_2O_3 on nanocrystalline hydroxyapatite bending strength and fracture toughness. Ceram. Int. 35, 1569–1574.

Morisue, H., Matsumoto, M., Chiba, K., Matsumoto, H., Toyama, Y., Aizawa, M., et al., 2009. Novel apatite fiber scaffolds can promote three-dimensional proliferation of osteoblasts in rodent bone regeneration models. J. Biomed. Mater. Res. A 90, 811–818.

Morrison, C.J., Gagnon, P., Cramer, S.M., 2011. Purification of monomeric mAb from associated aggregates using selective desorption chromatography in hydroxyapatite systems. Biotechnol. Bioeng. 108, 813–821.

Mukherjee, S., Kundu, B., Sen, S., Chanda, A., 2014. Improved properties of hydroxyapatite–carbon nanotube biocomposite: mechanical, in vitro bioactivity and biological studies. Ceram. Int. 40, 5635–5643.

Na, K., Kim, S.W., Sun, B.K., Woo, D.G., Yang, H.N., Chung, H.M., et al., 2007. Osteogenic differentiation of rabbit mesenchymal stem cells in thermo-reversible hydrogel constructs containing hydroxyapatite and bone morphogenic protein-2 (BMP-2). Biomaterials 28, 2631–2637.

Neira, I.S., Kolen'ko, Y.V., Kommareddy, K.P., Manjubala, I., Yoshimura, M., Guitian, F., 2010. Reinforcing of a calcium phosphate cement with hydroxyapatite crystals of various morphologies. ACS Appl. Mater. Interfaces 2, 3276–3284.

Ng, S., Guo, J., Ma, J., Loo, S.C.J., 2010. Synthesis of high surface area mesostructured calcium phosphate particles. Acta Biomater. 6, 3772–3781.

Notodihardjo, F.Z., Kakudo, N., Kushida, S., Suzuki, K., Kusumoto, K., 2012. Bone regeneration with BMP-2 and hydroxyapatite in critical-size calvarial defects in rats. J. Craniomaxillofac. Surg. 40, 287–291.

Okabayashi, R., Nakamura, M., Okabayashi, T., Tanaka, Y., Nagai, A., Yamashita, K., 2009. Efficacy of polarized hydroxyapatite and silk fibroin composite dressing gel on epidermal recovery from full-thickness skin wounds. J. Biomed. Mater. Res. B Appl. Biomater. 90, 641–646.

Porter, A.E., Patel, N., Skepper, J.N., Best, S.M., Bonfield, W., 2003. Comparison of in vivo dissolution processes in hydroxyapatite and silicon-substituted hydroxyapatite bioceramics. Biomaterials 24, 4609–4620.

Queiroz, A.C., Santos, J.D., Monteiro, F.J., Prado da Silva, M.H., 2003. Dissolution studies of hydroxyapatite and glass-reinforced hydroxyapatite ceramics. Mater. Charact. 50, 197–202.

Rodriguez-Ruiz, I., Delgado-Lopez, J.M., Duran-Olivencia, M.A., Iafisco, M., Tampieri, A., Colangelo, D., et al., 2013. pH-Responsive delivery of doxorubicin from citrate-apatite nanocrystals with tailored carbonate content. Langmuir 29, 8213–8221.

Rout, S.R., Behera, B., Maiti, T.K., Mohapatra, S., 2012. Multifunctional magnetic calcium phosphate nanoparticles for targeted platin delivery. Dalton Trans. 41, 10777–10783.

Sadat-Shojai, M., Khorasani, M.T., Dinpanah-Khoshdargi, E., Jamshidi, A., 2013. Synthesis methods for nanosized hydroxyapatite with diverse structures. Acta Biomater. 9, 7591–7621.

Sawyer, A.A., Weeks, D.M., Kelpke, S.S., McCracken, M.S., Bellis, S.L., 2005. The effect of the addition of a polyglutamate motif to RGD on peptide tethering to hydroxyapatite and the promotion of mesenchymal stem cell adhesion. Biomaterials 26, 7046–7056.

Shen, Y., Liu, J., Lin, K., Zhang, W., 2012. Synthesis of strontium substituted hydroxyapatite whiskers used as bioactive and mechanical reinforcement material. Mater. Lett. 70, 76–79.

Shin, Y., Aoki, H., Yoshiyama, N., Akao, M., Higashikata, M., 1992. Surface properties of hydroxyapatite ceramic as new percutaneous material in skin tissue. J. Mater. Sci. Mater. Med. 3, 219–221.

Suchanek, W., Yashima, M., Kakihana, M., Yoshimura, M., 1997. Hydroxyapatite–hydroxyapatite–whisker composites without sintering additives: mechanical properties and microstructural evolution. J. Am. Ceram. Soc. 80, 2805–2813.

Sun, W., Chu, C., Wang, J., Zhao, H., 2007. Comparison of periodontal ligament cells responses to dense and nanophase hydroxyapatite. J. Mater. Sci. Mater. Med. 18, 677–683.

Surmenev, R.A., Surmeneva, M.A., Ivanova, A.A., 2014. Significance of calcium phosphate coatings for the enhancement of new bone osteogenesis – a review. Acta Biomater. 10, 557–579.

Tadic, D., Peters, F., Epple, M., 2002. Continuous synthesis of amorphous carbonated apatites. Biomaterials 23, 2553–2559.

Uota, M., Arakawa, H., Kitamura, N., Yoshimura, T., Tanaka, J., Kijima, T., 2005. Synthesis of high surface area hydroxyapatite nanoparticles by mixed surfactant-mediated approach. Langmuir 21, 4724–4728.

Uskokovic, V., Uskokovic, D.P., 2011. Nanosized hydroxyapatite and other calcium phosphates: chemistry of formation and application as drug and gene delivery agents. J. Biomed. Mater. Res. B Appl. Biomater. 96, 152–191.

Valletregi, M., 2004. Calcium phosphates as substitution of bone tissues. Prog. Solid State Chem. 32, 1–31.

Wang, J., Shaw, L.L., 2009. Nanocrystalline hydroxyapatite with simultaneous enhancements in hardness and toughness. Biomaterials 30, 6565–6572.

Wang, D.G., Chen, C.Z., Ma, Q.S., Jin, Q.P., Li, H.C., 2013. A study on in vitro and in vivo bioactivity of HA/45S5 composite films by pulsed laser deposition. Appl. Surf. Sci. 270, 667–674.

Wu, L., Dou, Y., Lin, K., Zhai, W., Cui, W., Chang, J., 2011a. Hierarchically structured nanocrystalline hydroxyapatite assembled hollow fibers as a promising protein delivery system. Chem. Commun. (Camb.) 47, 11674–11676.

Wu, L., Dou, Y., Lin, K., Zhai, W., Cui, W., Chang, J., 2011b. Hierarchically structured nanocrystalline hydroxyapatite assembled hollow fibers as a promising protein delivery system. Chem. Commun. 47, 11674–11676.

Xia, L., Lin, K., Jiang, X., Xu, Y., Zhang, M., Chang, J., et al., 2013. Enhanced osteogenesis through nano-structured surface design of macroporous hydroxyapatite bioceramic scaffolds via activation of ERK and p38 MAPK signaling pathways. J. Mater. Chem. B 1, 5403–5416.

Xue, D., Zheng, Q., Zong, C., Li, Q., Li, H., Qian, S., et al., 2010. Osteochondral repair using porous poly(lactide-co-glycolide)/nano-hydroxyapatite hybrid scaffolds with undifferentiated mesenchymal stem cells in a rat model. J. Biomed. Mater. Res. A 94, 259–270.

Yu, H., VandeVord, P.J., Mao, L., Matthew, H.W., Wooley, P.H., Yang, S.Y., 2009. Improved tissue-engineered bone regeneration by endothelial cell mediated vascularization. Biomaterials 30, 508–517.

Yuan, H., Fernandes, H., Habibovic, P., Boer, J.d., Barradas, A.M.C., Ruiter, A.d., et al., 2010. Osteoinductive ceramics as a synthetic alternative to autologous bone grafting. Proc. Natl. Acad. Sci. U. S. A. 107, 13614–13619.

Zhang, N., Zhai, D., Chen, L., Zou, Z., Lin, K., Chang, J., 2014. Hydrothermal synthesis and characterization of Si and Sr co-substituted hydroxyapatite nanowires using strontium containing calcium silicate as precursors. Mater. Sci. Eng. C: Mater. Biol. Appl. 37, 286–291.

Zhou, H., Lee, J., 2011. Nanoscale hydroxyapatite particles for bone tissue engineering. Acta Biomater. 7, 2769–2781.

Zhou, C., Hong, Y., Zhang, X., 2013. Applications of nanostructured calcium phosphate in tissue engineering. Biomater. Sci. 1, 1012–1028.

Zhu, S.H., Huang, B.Y., Zhou, K.C., Huang, S.P., Liu, F., Li, Y.M., et al., 2004. Hydroxyapatite nanoparticles as a novel gene carrier. J. Nanopart. Res. 6, 307–311.

Zou, Z., Lin, K., Chen, L., Chang, J., 2012. Ultrafast synthesis and characterization of carbonated hydroxyapatite nanopowders via sonochemistry-assisted microwave process. Ultrason. Sonochem. 19, 1174–1179.